

# Optimizing Ultra-Reliable and Low-Latency Communication Systems with Unsupervised Learning

Chengjian Sun, Changyang She and Chenyang Yang

## Abstract

Supervised learning has been introduced to wireless communications to solve complex problems due to its wide applicability. However, generating labels for supervision could be expensive or even unavailable in wireless communications, and constraints cannot be explicitly guaranteed in the supervised manner. In this work, we introduced an unsupervised learning framework, which exploits mathematic models and the knowledge of optimization to search an unknown policy without supervision. Such a framework is applicable to both variable and functional optimization problems with instantaneous and long-term constraints. We take two resource allocation problems in ultra-reliable and low-latency communications as examples, which involve one and two timescales, respectively. Unsupervised learning is adopted to find the approximated optimal solutions of the problems. Simulation results show that the learned solution can achieve the same bandwidth efficiency as the optimal solution in the symmetric scenarios. By comparing the learned solution with the existing policies, our results illustrate the benefit of exploiting frequency diversity and multi-user diversity in improving the bandwidth efficiency in both symmetric and asymmetric scenarios. We further illustrate that, with pre-training, the unsupervised learning algorithm converges rapidly.

## Index Terms

Unsupervised learning, ultra-reliable and low-latency communications, constraints, neural networks, resource allocation

This paper has been presented in part at the IEEE Global Communications Conference 2019 [1].

C. Sun and C. Yang are with the School of Electronics and Information Engineering, Beihang University, Beijing 100191, China (email: {sunchengjian, cyyang}@buaa.edu.cn).

C. She is with the School of Electrical and Information Engineering, University of Sydney, Sydney, NSW 2006, Australia (e-mail: shechangyang@gmail.com).

## I. INTRODUCTION

### A. Background and Motivation

Beyond fifth generation (5G) communication systems are expected to support emerging applications with diverse quality-of-service (QoS) requirements, including enhanced mobile broadband services, massive machine-type communications, and ultra-reliable and low-latency communications (URLLC) [2]. To ensure the QoS requirements in a dynamic wireless network, a base station (BS) has to adjust its strategies (such as resource allocation, precoding matrices, coding and modulation schemes, schedulers and handover strategies) according to the dynamic environment. With traditional optimization algorithms, the BS needs to execute these algorithms every few milliseconds, depending on the channel coherence time. This will bring high computing overheads. In addition, if the processing delay for searching the optimal solution is longer than channel coherence time, the obtained solution cannot guarantee the QoS requirements with the current channel realization. This issue is critical in 5G systems, especially for URLLC [3].

To avoid executing searching algorithms when the environment parameters change, one needs the closed-form expression of a policy, which is a function that maps the environmental parameters of the wireless network to the optimal decision. An optimization problem that optimizes the expression of a function belongs to functional optimization problems [4], where the optimization variable is a function rather than a vector in traditional optimization problems. In general, one can hardly derive a closed-form solution of a functional optimization problem. One of the widely applied numerical methods for solving functional optimization problems is finite element method (FEM) [5]. As a mesh-based method, FEM suffers from the curse of dimensionality, especially in the multi-user scenarios in wireless networks, where the dimension increases with the number of users. To overcome this difficulty, we approximate the optimal policy with a deep neural network (DNN), and optimizing the parameters of the DNN [6]. According to the universal approximation theorem in [7], a continuous and deterministic function (e.g., an optimal policy in 5G systems) can be approximated by a feed-forward neural network arbitrarily well.

### B. Related Works

In the existing literature, two branches of deep learning algorithms are used in wireless networks: supervised deep learning [8–11] and deep reinforcement learning [12, 13].

Based on the universal approximation theorem, the authors of [8] further proved that a multi-layer feed-forward neural network is an universal approximator of iterative algorithms. Thus, one

can obtain near-optimal solutions from DNNs rather than iterative algorithms that are general with high complexity. A deep learning framework was proposed in [10] to find the latent relationship between flow information and link usage by learning from past computation experience. To learn the optimal predictive resource allocation under the QoS constraint of video-on-demand service, a deep neural network (DNN) was designed in [9]. To improve the approximation accuracy, a cascaded neural network was introduced to approximate optimal resource allocation policies and deep transfer learning was applied to fine-tune the DNN in non-stationary wireless networks [11]. By training the DNNs offline, an approximated decision can be obtained with low complexity online [8–11], say about 1% of the original numerical optimization [9]. Such an idea of “learning to optimize” can be regarded as a kind of computing offloading over time, which shifts the computations from online to offline. However, there are two open problems in supervised deep learning: 1) the optimization algorithm that can find the labels may not be available. 2) It is not clear whether the approximated decision can guarantee the QoS requirements with high probability.

In [12, 13], reinforcement learning was employed to solve the multi-timescale optimization problems in URLLC, where channel allocation and scheduling policies were learned according to the states of packet loss rate and the age of information, respectively. With deep reinforcement learning, the agent (e.g., the BS or a centralized control plane) learns how to make decision from the feedback of the environment, where a DNN is used to approximate a good policy obtained from exploration [12, 13]. Although no labeled training sample is needed in deep reinforcement learning, the agent needs to explore decisions in unknown environment to improve the long-term reward. As a result, it may try a bad decision in a time slot and cannot guarantee instantaneous constraints in wireless networks.

### *C. Our Contributions*

To address the issues in supervised deep learning and deep reinforcement learning, we study how to optimize B5G systems with unsupervised deep learning that does not require labeled training samples. Essentially, unsupervised deep learning trains DNNs from the property of the models. In our framework, we train DNNs from the Karush-Kuhn-Tucker (KKT) conditions of a problem. The main contributions of this paper are summarized as follows.

- We develop a framework that applies unsupervised deep learning to find the numerical approximation of the optimal policy subject to short-term instantaneous constraints and long-

term statistic constraints, where these constraints vary according to environment parameters in dynamic wireless networks.

- We prove that a traditional variable optimization problem is equivalent to a functional optimization problem. By solving the functional optimization problem, our framework can obtain the approximated optimal policy (i.e., a well-trained DNN) of the original variable optimization problem.
- In an example system, we show how to apply the framework in downlink (DL) resource allocation for URLLC. In the systems with constant power allocation, the DNN that maps the large-scale channel gains and the bandwidth allocation is obtained. In the systems that allocate transmit power according to small-scale channel gains, we obtain the DNN that approximates the optimal power control policy.
- In a symmetric scenario that the QoS requirements and the large-scale channel gains of all the users are identical, we derive the closed-form expression of the optimal power control policy. Simulation and numerical results show that performance of the DNN is very close to that of the closed-form optimal policy. In addition, the output of DNN can guarantee the QoS requirements of URLLC with high probability.

The rest of the paper is organized as follows. In Section II, we show how to transfer a variable optimization problem to a functional optimization problem and how to solve functional optimization problems with unsupervised deep learning. In Section III, we formulate the system model of URLLC in a cellular network. We illustrate how to use unsupervised deep learning to find an approximation of optimal bandwidth allocation policy and an approximation of optimal power allocation policy in Section IV and Section V, respectively. Simulation and numerical results are provided in Section VI. We conclude this paper in Section VII.

## II. UNSUPERVISED DEEP LEARNING FOR SOLVING FUNCTIONAL OPTIMIZATION PROBLEMS

In this section, we first discuss the relation between variable and functional optimization problems. Then, we summarize some typical constrained functional optimization problems in wireless networks. Finally, we show how to solve functional optimization problems with unsupervised deep learning.

### A. Functional Optimization Problems with Instantaneous Constraints

Consider a general variable optimization problem that optimizes a vector  $\mathbf{x} \in \mathcal{D}_x \subseteq \mathbb{R}^{N_x}$  consisting of  $N_x$  variables,

$$\min_{\mathbf{x}} f(\mathbf{x}; \boldsymbol{\theta}) \quad (1)$$

$$\text{s.t. } C_i(\mathbf{x}; \boldsymbol{\theta}) \leq 0, i = 1, \dots, I, \quad (1a)$$

where  $\boldsymbol{\theta} \in \mathcal{D}_\theta \subseteq \mathbb{R}^{N_\theta}$  is a vector of  $N_\theta$  environmental parameters such as channel gains. The elements of  $\boldsymbol{\theta}$  are random variables with probability density function (PDF)  $p(\boldsymbol{\theta}) \geq 0$ .  $f(\mathbf{x}; \boldsymbol{\theta}) : \mathcal{D}_x \times \mathcal{D}_\theta \mapsto \mathbb{R}$  and  $C_i(\mathbf{x}; \boldsymbol{\theta}) : \mathcal{D}_x \times \mathcal{D}_\theta \mapsto \mathbb{R}$  are the objective function and  $I$  constraint functions of  $\mathbf{x}$  and  $\boldsymbol{\theta}$ , respectively. We assume that  $\mathcal{D}_\theta$  is a compact set and  $f(\mathbf{x}; \boldsymbol{\theta})$  and  $C_i(\mathbf{x}; \boldsymbol{\theta})$  are differentiable with respect to (w.r.t.)  $\mathbf{x}$  and  $\boldsymbol{\theta}$ . Since the constraint  $\mathbf{x} \in \mathcal{D}_x$  does not depend on  $\boldsymbol{\theta}$ , it is a deterministic constraint, which can be considered as a special case of the constraints in (1a). Thus, we remove  $\mathbf{x} \in \mathcal{D}_x$  from the optimization problem in the sequel.

The function that maps  $\boldsymbol{\theta}$  to the optimal solution of problem (1) is denoted by  $\mathbf{x}^* = f_0(\boldsymbol{\theta}) : \mathcal{D}_\theta \mapsto \mathcal{D}_x$ . In most of the cases, we can hardly derive the closed-form expression of  $f_0(\boldsymbol{\theta})$ . As a result, the system needs to solve problem (1) numerically whenever  $\boldsymbol{\theta}$  changes. Due to high computing overheads for executing optimization algorithms, this approach can hardly be implemented in real-world communication systems, especially for the services with stringent delay requirements.

To address this issue, we turn to a functional optimization problem that optimizes the relation between  $\mathbf{x}$  and  $\boldsymbol{\theta}$ ,

$$\min_{\mathbf{x}(\boldsymbol{\theta})} \int_{\boldsymbol{\theta} \in \mathcal{D}_\theta} f[\mathbf{x}(\boldsymbol{\theta}); \boldsymbol{\theta}] p(\boldsymbol{\theta}) d\boldsymbol{\theta} \quad (2)$$

$$\text{s.t. } C_i[\mathbf{x}(\boldsymbol{\theta}); \boldsymbol{\theta}] \leq 0, \forall \boldsymbol{\theta} \in \mathcal{D}_\theta, i = 1, \dots, I, \quad (2a)$$

where  $\mathbf{x}(\boldsymbol{\theta})$  is optimized to minimize the expectation of the objective function in problem (1) over  $\boldsymbol{\theta}$ . It is worth noting that constraints in (1a) and (2a) are different. In a variable optimization problem, we only need to ensure constraints in (1a) for a certain realization of  $\boldsymbol{\theta}$ . However, in a functional optimization problem, we need to ensure constraints in (2a) for all the possible values of  $\boldsymbol{\theta} \in \mathcal{D}_\theta$ . In other words, each constraint in (2a) is equivalent to infinite constraints in (1a).

**Proposition 1.** Problem (1) and problem (2) are equivalent in the sense that the optimal solutions

of problem (1) are the optimal solutions of problem (2); with probability one, the optimal solutions of problem (2) are optimal for problem (1).

*Proof.* See proof in Appendix A. □

According to Proposition 1, if we can derive the optimal solution of problem (2), denoted by  $\mathbf{x}_{\text{opt}}(\boldsymbol{\theta})$ , then with probability one,  $\mathbf{x}_{\text{opt}}(\boldsymbol{\theta})$  is the optimal solution of problem (1).

The constraints in problems (1) and (2) depend on the instantaneous values of the environmental parameters, and hence we refer to them as instantaneous constraints.

### B. Functional Optimization Problems with Statistic Constraints

Some problems in wireless networks are naturally formulated as constrained functional optimization problems, rather than the variable optimization problem in (1). For example, the problem that maximizes the average throughput of a fading channel subject to the average transmit power constraint [14],

$$\begin{aligned} \max_{P(g)} \quad & \int_0^{\infty} W \log_2 \left[ 1 + \frac{\alpha g P(g)}{N_0 W} \right] p(g) dg, & (3) \\ \text{s.t.} \quad & \int_0^{\infty} P(g) p(g) dg \leq P_{\text{ave}}, & (3a) \end{aligned}$$

where  $W$  is the bandwidth,  $\alpha$  is the large-scale channel gain,  $g$  is the small-scale channel gain,  $N_0$  is the single-side noise spectral density,  $P_{\text{ave}}$  is the average transmit power of the transmitter, and  $p(g)$  is the pdf of the small-scale channel gain. In problem (3), we optimize the power control policy  $P(g)$ . Once  $P(g)$  is obtained, the transmitter can adjust the transmit power according to the small-scale channel gain.

In problem (3), the small-scale channel gain is the environmental parameter and the transmit power allocation policy is the optimization variable. Owing to the long-term statistic constraint on the average transmit power, we cannot formulate problem (3) as a variable optimization problem in (1) or the functional optimization problem in (2). The difference between them lies in the constraints. Unlike instantaneous constraints, the constraints in (3a) rely on the distribution of the environmental parameter, but does not depend on the observed value of  $g$ . We refer this kind of constraints as statistic constraint.

### C. Unsupervised Deep Learning for Solving Functional Optimization Problems

A functional optimization problem with both instantaneous and statistic constraints can be expressed as follows,

$$\min_{\mathbf{x}(\boldsymbol{\theta})} \mathbb{E}_{\boldsymbol{\theta}}\{f[\mathbf{x}(\boldsymbol{\theta}), \boldsymbol{\theta}]\} \quad (4)$$

$$\text{s.t. } C_i[\mathbf{x}(\boldsymbol{\theta}), \boldsymbol{\theta}] \leq 0, \forall \boldsymbol{\theta} \in \mathcal{D}_{\theta}, i = 1, \dots, I, \quad (4a)$$

$$\mathbb{E}_{\boldsymbol{\theta}}\{C_j[\mathbf{x}(\boldsymbol{\theta}), \boldsymbol{\theta}]\} \leq 0, j = I + 1, \dots, I + J, \quad (4b)$$

where  $J$  is the number of statistic constraints.

To find the optimal solution of problem (4), we first define the Lagrangian of the problem as

$$\begin{aligned} L \triangleq & \int_{\boldsymbol{\theta} \in \mathcal{D}_{\theta}} f[\mathbf{x}(\boldsymbol{\theta}), \boldsymbol{\theta}] p(\boldsymbol{\theta}) d\boldsymbol{\theta} \\ & + \sum_{i=1}^I \int_{\boldsymbol{\theta} \in \mathcal{D}_{\theta}} \lambda_i(\boldsymbol{\theta}) C_i[\mathbf{x}(\boldsymbol{\theta}), \boldsymbol{\theta}] d\boldsymbol{\theta} + \sum_{j=I+1}^{I+J} \nu_j \int_{\boldsymbol{\theta} \in \mathcal{D}_{\theta}} C_j[\mathbf{x}(\boldsymbol{\theta}), \boldsymbol{\theta}] p(\boldsymbol{\theta}) d\boldsymbol{\theta} \end{aligned} \quad (5)$$

where  $\lambda_i(\boldsymbol{\theta}) \geq 0, \forall \boldsymbol{\theta} \in \mathcal{D}_{\theta}$ , and  $\nu_j \geq 0$  are the Lagrange multipliers. For all the possible values of  $\boldsymbol{\theta}$ , constraints in (4a) should be satisfied. Thus, the related Lagrange multipliers  $\lambda_i(\boldsymbol{\theta})$  is a function w.r.t.  $\boldsymbol{\theta}$ .

1) *Theoretical Approach:* The optimal solution of problem (4) should satisfy the following necessary conditions [15],

$$\frac{\delta L}{\delta \mathbf{x}(\boldsymbol{\theta})} \triangleq \frac{\partial f[\mathbf{x}(\boldsymbol{\theta}), \boldsymbol{\theta}]}{\partial \mathbf{x}(\boldsymbol{\theta})} p(\boldsymbol{\theta}) + \sum_{i=1}^I \lambda_i(\boldsymbol{\theta}) \frac{\partial C_i[\mathbf{x}(\boldsymbol{\theta}), \boldsymbol{\theta}]}{\partial \mathbf{x}(\boldsymbol{\theta})} + \sum_{j=I+1}^{I+J} \nu_j \frac{\partial C_j[\mathbf{x}(\boldsymbol{\theta}), \boldsymbol{\theta}]}{\partial \mathbf{x}(\boldsymbol{\theta})} p(\boldsymbol{\theta}) = \mathbf{0}, \forall \boldsymbol{\theta} \in \mathcal{D}_{\theta}, \quad (6)$$

$$\lambda_i(\boldsymbol{\theta}) C_i[\mathbf{x}(\boldsymbol{\theta}), \boldsymbol{\theta}] = 0, \forall \boldsymbol{\theta} \in \mathcal{D}_{\theta}, \quad (7)$$

$$\nu_j \mathbb{E}_{\boldsymbol{\theta}}\{C_j[\mathbf{x}(\boldsymbol{\theta}), \boldsymbol{\theta}]\} = 0, \quad (8)$$

$$\lambda_i(\boldsymbol{\theta}) \geq 0, \forall \boldsymbol{\theta} \in \mathcal{D}_{\theta}, \nu_j \geq 0, \quad (9)$$

$$(4a), (4b), \forall \boldsymbol{\theta} \in \mathcal{D}_{\theta},$$

where (6) is the simplified form of the Euler-Lagrange equation, i.e., (3.9) in [16]. Since the above necessary conditions are in the same spirit as the KKT conditions of variable optimization problems, we refer to them as KKT conditions of functional optimization problems.

Deriving the expression of the optimal solution from the KKT conditions is very challenging. This is because the KKT conditions are multi-dimensional partial differential equations. In the rest part of this section, we introduce a numerical approach to solve problem (4).

2) *Numerical Approach:* When problem (4) is convex<sup>1</sup> and the Slater's condition holds, problem (4) is equivalent to the following problem [15, 17],

$$\begin{aligned} \max_{\lambda_i(\boldsymbol{\theta}), \nu_j} \min_{\boldsymbol{x}(\boldsymbol{\theta})} L & \quad (10) \\ \text{s.t. (9)} & \end{aligned}$$

**Remark 1.** The convexity of problem (4) and the Slater's condition are sufficient conditions for the equivalence. If the problem is non-convex, by solving problem (10) we can obtain a local optimal solution of problem (4) [18].

According to the Universal Approximation Theory of deep neural networks (DNNs), a deterministic continuous function defined over a compact set can be approximated by a DNN, and the approximation can be arbitrarily accurate [7, 19]. Thus, we can approximate  $\boldsymbol{x}(\boldsymbol{\theta})$  and  $\boldsymbol{\lambda}(\boldsymbol{\theta}) \triangleq [\lambda_1(\boldsymbol{\theta}), \dots, \lambda_I(\boldsymbol{\theta})]^T$  with two DNNs, denoted by  $\mathcal{N}_x(\boldsymbol{\theta}; \boldsymbol{\omega}_x)$  and  $\mathcal{N}_\lambda(\boldsymbol{\theta}; \boldsymbol{\omega}_\lambda)$ , respectively, where  $\boldsymbol{\omega}_x$  and  $\boldsymbol{\omega}_\lambda$  are the parameters of them.

By replacing  $\boldsymbol{x}(\boldsymbol{\theta})$  and  $\boldsymbol{\lambda}(\boldsymbol{\theta})$  with  $\hat{\boldsymbol{x}}(\boldsymbol{\theta}) \triangleq \mathcal{N}_x(\boldsymbol{\theta}; \boldsymbol{\omega}_x)$  and  $\hat{\boldsymbol{\lambda}}(\boldsymbol{\theta}) \triangleq \mathcal{N}_\lambda(\boldsymbol{\theta}; \boldsymbol{\omega}_\lambda)$ , problem (10) can be re-written as,

$$\max_{\boldsymbol{\omega}_\lambda, \nu_j} \min_{\boldsymbol{\omega}_x} \hat{L} = \mathbb{E}_\theta \left\{ f[\hat{\boldsymbol{x}}(\boldsymbol{\theta}), \boldsymbol{\theta}] + \sum_{j=I+1}^{I+J} \nu_j \{C_j[\hat{\boldsymbol{x}}(\boldsymbol{\theta}), \boldsymbol{\theta}]\} \right\} + \sum_{i=1}^I \int_{\boldsymbol{\theta} \in \mathcal{D}_\theta} \hat{\lambda}_i(\boldsymbol{\theta}) C_i[\hat{\boldsymbol{x}}(\boldsymbol{\theta}), \boldsymbol{\theta}] d\boldsymbol{\theta} \quad (11)$$

$$\text{s.t. } \hat{\lambda}_i(\boldsymbol{\theta}) \geq 0, \forall \boldsymbol{\theta} \in \mathcal{D}_\theta, \nu_j \geq 0. \quad (11a)$$

To find a solution of problem (11), we apply the primal-dual method to update between primal variables  $\boldsymbol{\omega}_x$  and dual variables  $\boldsymbol{\omega}_\lambda$  and  $\nu_j$  iteratively [20, 21]. Let  $\boldsymbol{\omega}_x^{(t)}$ ,  $\boldsymbol{\omega}_\lambda^{(t)}$  and  $\nu_j^{(t)}$  denote the evaluated values of  $\boldsymbol{\omega}_x$ ,  $\boldsymbol{\omega}_\lambda$  and  $\nu_j$  at the  $t$ th iteration. Then, these variables can be updated by the stochastic gradient descent (SGD) method and the stochastic gradient ascent (SGA) method

<sup>1</sup>The objective function and the left-hand-sides (LHS) of constraints (4a) and (4b) are convex in  $\boldsymbol{x}(\boldsymbol{\theta})$ , and  $\mathcal{D}_x$  is a convex set.

according to

$$\boldsymbol{\omega}_x^{(t+1)} = \boldsymbol{\omega}_x^{(t)} - \eta_{\omega_x} \nabla_{\omega_x} \hat{L}, \quad (12)$$

$$\boldsymbol{\omega}_\lambda^{(t+1)} = \boldsymbol{\omega}_\lambda^{(t)} + \eta_{\omega_\lambda} \nabla_{\omega_\lambda} \hat{L}, \quad (13)$$

$$\nu_j^{(t+1)} = \left( \nu_j^{(t)} + \eta_{\nu_j} \frac{\partial \hat{L}}{\partial \nu_j} \right)^+, \quad (14)$$

where  $(x)^+ \triangleq \max\{x, 0\}$  ensures  $\nu_j^{(t+1)}$  to be positive,  $\eta_{\omega_x}$ ,  $\eta_{\omega_\lambda}$  and  $\eta_{\nu_j}$  are the learning rates for updating  $\boldsymbol{\omega}_x$ ,  $\boldsymbol{\omega}_\lambda$  and  $\nu_j$ , respectively, and  $\nabla_{\omega_x} \hat{L}$  and  $\nabla_{\omega_\lambda} \hat{L}$  denote the gradients of  $\hat{L}$  w.r.t.  $\omega_x$  and  $\omega_\lambda$ , respectively<sup>2</sup>. To guarantee  $\hat{\lambda}_i(\boldsymbol{\theta}) \geq 0, \forall \boldsymbol{\theta} \in \mathcal{D}_\theta$ , we need to choose a proper activation function in the output layer of  $\mathcal{N}_\lambda(\boldsymbol{\theta}; \boldsymbol{\omega}_\lambda)$ , e.g.  $\text{ReLU}(x) \triangleq \max(x, 0)$  or  $\text{SoftPlus}(x) \triangleq \ln[1 + \exp(x)]$  [22,23]. The method to compute (12), (13) and (14) is provided in Appendix B.

**Remark 2.** To train the DNNs, we optimize  $\boldsymbol{\omega}_x$ ,  $\boldsymbol{\omega}_\lambda$ ,  $\nu_j$ ,  $j = I + 1, \dots, I + J$ , with the SGD method and the SGA method. As shown in [20], the primal-dual method converges to a local optimal solution of problem (11). A local optimal solution is either at a stationary point of  $\hat{L}$  or on the boundary of the feasible region. Thus, the following properties hold at local optimal solutions:  $\nabla_{\omega_x} \hat{L} = \mathbf{0}$ ,  $\nabla_{\omega_\lambda} \hat{L} = \mathbf{0}$  (or  $\hat{\lambda}_i(\boldsymbol{\theta}) = 0$ ) and  $\partial \hat{L} / \partial \nu_j = 0$  (or  $\nu_j = 0$ ),  $j = I + 1, \dots, I + J$ . These properties implicitly serve as the ‘‘supervised signal’’ of the DNNs. Since this learning method does not need labeled training sample, it belongs to unsupervised deep learning.

### III. ULTRA-RELIABLE AND LOW-LATENCY COMMUNICATIONS

In the rest part of this work, we take URLLC as an example to illustrate how to apply unsupervised deep learning.

#### A. System Model

Consider a DL orthogonal frequency division multiple access system, where a BS with  $N_t$  antennas serves  $K$  single-antenna users. The maximal transmit power and the total bandwidth of the BS are denoted by  $P_{\max}$  and  $W_{\max}$ , respectively. Packets for each user arrive at the buffer of the BS randomly. The inter-arrival time between packets could be shorter than the service time of each packet. Therefore, the packets may wait in the buffer of the BS. We consider a queueing

<sup>2</sup>The gradient of a scalar  $x$  w.r.t. to a vector  $\mathbf{y}_{N_y \times 1}$  is defined as  $\nabla_{\mathbf{y}} x \triangleq [\partial x / \partial y_1, \dots, \partial x / \partial y_{N_y}]^T$  and the gradient of a vector  $\mathbf{x}_{N_x \times 1}$  w.r.t. to a vector  $\mathbf{y}_{N_y \times 1}$  is defined as  $\nabla_{\mathbf{y}} \mathbf{x} \triangleq [\nabla_{\mathbf{y}} x_1, \dots, \nabla_{\mathbf{y}} x_{N_x}]$ .

model that the packets for different users wait in different queues and are served according to first-come-first-serve order.

### B. Quality-of-Service Requirement

The QoS requirements of URLLC can be characterized by the delay bound  $D_{\max}$  and the overall packet loss probability  $\varepsilon_{\max}$ . The uplink transmission delay, backhaul delay and processing delay have been studied in [24], [25] and [26], respectively, and are subtracted from the E2E delay in this paper. Thus, herein  $D_{\max}$  is the DL delay, which consists of the queueing delay (denoted as  $D_k^q$  for the  $k$ th user), transmission delay  $D^t$  and decoding delay  $D^c$ . All these delay components are measured in slots.  $D^t$  and  $D^c$  are constant values [27]. Due to the random packet arrival,  $D_k^q$  is random. To ensure the delay requirement,  $D_k^q$  should be bounded by  $D_{\max}^q \triangleq D_{\max} - D^t - D^c$ . If the queueing delay of a packet exceeds  $D_{\max}^q$ , the packet will be useless.

### C. Channel Model

Since the packet size  $u$  in URLLC is typically small (e.g., 20 bytes or 32 bytes [2]), the bandwidth required for transmitting each packet is less than the channel coherence bandwidth. Therefore, the channel is flat fading. Time is discretized into slots, each with duration  $T_s$ . The duration for DL data transmission in one slot is  $\tau$  and the duration for channel training is  $T_s - \tau$ . Since the E2E delay requirement in URLLC is typically shorter than the channel coherence time, the channel is quasi-static and time diversity cannot be exploited. To guarantee the transmission reliability within the delay bound, we consider frequency hopping, where each user is assigned with different subchannels in adjacent slots. When the frequency interval between adjacent subchannels is larger than the coherence bandwidth, the small-scale channel gains of a user among slots are mutual independent.

As shown in [14], the large-scale channel gain of a user varies when the moving distance of the user is comparable to the decorrelation distance of shadowing, i.e., 50 ~ 100 m. Thus, the large-scale channel gain may remain constant in a few second, which is much longer than the required delay bound  $D_{\max}^q$  and  $T_s$  (e.g., in 5G New Radio,  $T_s$  can be much shorter than 1 ms [28]). We assume that large-scale channel gains stay constant in each frame that consists of  $N_f$  time slots, and vary in different frames. The relations among slots, frames, and the required delay bound are illustrated in Fig. 1.

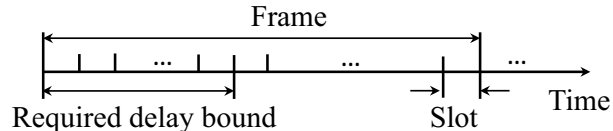


Fig. 1. Relations among slots, frames, and the required delay bound.

#### D. Achievable Rate in Finite Blocklength Regime

In URLLC, the blocklength of channel coding is short due to the short transmission duration, and hence the impact of decoding errors on reliability cannot be ignored. Since Shannon's capacity formula cannot be employed to characterize the probability of decoding errors [29], we consider the achievable rate in finite blocklength regime. In quasi-static flat fading channels, when channel state information is available at the transmitter and receiver, the achievable rate of the  $k$ th user (in packets/slot) can be accurately approximated by [30],

$$s_k \approx \frac{\tau W_k}{u \ln 2} \left[ \ln \left( 1 + \frac{\alpha_k g_k P_k}{N_0 W_k} \right) - \sqrt{\frac{V_k}{\tau W_k}} Q_G^{-1}(\varepsilon_k^c) \right], \quad (15)$$

where  $W_k$  and  $P_k$  are the bandwidth and the transmit power allocated to the  $k$ th user, respectively,  $\varepsilon_k^c$  is the decoding error probability of the  $k$ th user,  $\alpha_k$  and  $g_k$  are the large-scale channel gain and small-scale channel gain of the  $k$ th user, respectively,  $Q_G^{-1}(x)$  is the inverse of the Gaussian Q-function, and  $V_k$  is the channel dispersion given by [30],

$$V_k = 1 - \frac{1}{\left[ 1 + \frac{\alpha_k g_k P_k}{N_0 W_k} \right]^2}. \quad (16)$$

Although the achievable rate is in closed-form, it is still too complicated to obtain graceful results. As shown in [29], if the signal-to-noise ratio (SNR)  $\frac{\alpha_k g_k P_k}{N_0 W_k} \geq 5$  dB,  $V_k \approx 1$  is accurate. Since high SNR is required to ensure ultra-high reliability and ultra-low latency, such approximation is reasonable. Even when the SNR is not high, we can obtain a lower bound of the achievable rate by substituting  $V_k \approx 1$  into  $s_k$ . Then, when the required  $\varepsilon^c$  is satisfied with the lower bound, it can also be satisfied with the achievable rate in (15).

Denote  $\varepsilon_k^q \triangleq \Pr\{D_k^q > D_{\max}^q\}$  as the queueing delay violation probability. Then, the overall reliability requirement can be characterized by

$$1 - (1 - \varepsilon_k^c)(1 - \varepsilon_k^q) \approx \varepsilon_k^c + \varepsilon_k^q \leq \varepsilon_{\max}. \quad (17)$$

This approximation is very accurate, because the values of  $\varepsilon^c$  and  $\varepsilon^q$  are very small in URLLC. The results in [24, 31] show that the optimal values of  $\varepsilon_k^c$  and  $\varepsilon_k^q$  are in the same order of magnitude. In the example, we set  $\varepsilon_k^c = \varepsilon_k^q = \varepsilon_{\max}/2$  for simplicity.

### E. Effective Bandwidth and Effective Capacity for Queue Delay Analysis

Effective bandwidth and effective capacity have been widely used to analyze the tail probability of queueing delay, i.e.,  $D_{\max}^q$  is large or  $\varepsilon_k^q$  is extremely small [32, 33]. Effective bandwidth of a packet arrival process is the minimal constant packet service rate that is required to guarantee the delay bound and the delay bound violation probability,  $D_{\max}^q$  and  $\varepsilon_k^q$  [32]. Effective capacity of a packet service process is the maximal constant packet arrival rate that can be supported by the service process subjected to the requirements on the delay bound and the delay bound violation [33].

Take the Poisson arrival process with the average packet arrival rate  $a_k$  packets/slot as an example, whose effective bandwidth can be expressed as [31]

$$B_k^E = \frac{\ln(\varepsilon_{\max}/2)}{D_{\max}^q \ln\left[1 - \frac{\ln(\varepsilon_{\max}/2)}{a_k D_{\max}^q}\right]} \text{ (packets/slot)}. \quad (18)$$

If the constant packet service rate is equal to or higher than  $B_k^E$ , then we have<sup>3</sup>

$$\Pr\{D_k^q > D_{\max}^q\} \leq \exp\{-\vartheta_k B_k^E D_{\max}^q\}. \quad (19)$$

where  $\vartheta_k$  is the QoS component, which reflects the decay rate of the tail probability of the queueing delay. By setting the upper bound in (19) equals to  $\varepsilon_{\max}/2$ , we can obtain that

$$\vartheta_k = \ln\left[1 - \frac{\ln(\varepsilon_{\max}/2)}{a_k D_{\max}^q}\right]. \quad (20)$$

Since the small-scale channel gains of a user are independent among slots owing to frequency hopping, the effective capacity of the  $k$ th user can be expressed as [34]

$$C_k^E = -\frac{1}{\vartheta_k} \ln \mathbb{E}_{\mathbf{g}} \{e^{-\vartheta_k s_k}\} \text{ (packets/slot)}, \quad (21)$$

where the expectation is taken over the small-scale channel gains,  $\mathbf{g} \triangleq (g_1, g_2, \dots, g_K) \in \mathbb{R}_+^K$ .

<sup>3</sup>As analyzed in [31], if the slot duration is much shorter than the delay bound, which is true in URLLC, effective bandwidth can be used to analyze the queueing delay at the BS for Poisson, interrupted Poisson and switched Poisson arrival processes.

When both the packet arrival process and the packet service process are stochastic,  $D_{\max}^q$  and  $\varepsilon_k^q$  can be satisfied if [35]

$$C_k^E \geq B_k^E. \quad (22)$$

#### F. Minimizing the Occupied Bandwidth

In 5G systems, there are different kinds of services. Since URLLC has stringent QoS requirements, the priority of URLLC is higher than the other kinds of services. By minimizing the total bandwidth occupied by URLLC subject to its' QoS requirements, we maximize the residual bandwidth for the rest of the services. In the next two sections, we minimize the bandwidth occupied by URLLC by optimizing bandwidth allocation with or without dynamic power control.

### IV. BANDWIDTH ALLOCATION WITHOUT DYNAMIC POWER CONTROL

In this section, we assume that the total transmit power of the BS is equally allocated in the frequency domain and does not change according to the small-scale channel gains, i.e.,  $P_0 \triangleq P_{\max}/W_{\max}$ . Such an assumption is reasonable in practical cellular network [36]. In addition, the analysis in [14] shows that the equal power allocation policy is near optimal in high SNR regime. With this assumption, we illustrate how to reformulate a variable optimization problem as a functional optimization problem with instantaneous constraints.

#### A. Problem Formulation

By substituting  $P_0 = P_{\max}/W_{\max}$  into (15), the achievable rate can be re-written as follows,

$$s_k = \frac{\tau W_k}{u \ln 2} \left[ \ln \left( 1 + \frac{\alpha_k g_k}{N_0} P_0 \right) - \frac{Q_G^{-1}(\varepsilon_{\max}/2)}{\sqrt{\tau W_k}} \right]. \quad (23)$$

For given large scale channel gains, the optimal bandwidth allocation problem that minimizes the total bandwidth required to ensure the QoS of every user can be formulated as,

$$\min_{W_k, k=1, \dots, K} \sum_{k=1}^K W_k \quad (24)$$

$$\text{s.t. } \mathbb{E}_{g_k} \{ e^{-\vartheta_k s_k} \} - e^{-\vartheta_k B_k^E} \leq 0, k = 1, \dots, K \quad (24a)$$

$$\sum_{k=1}^K W_k \leq W_{\max}, \quad (24b)$$

$$(23), W_k > 0, k = 1, \dots, K.$$

where (24a) is obtained by substituting (21) into the QoS constraint in (22), and (24b) is the total bandwidth constraint. Since the transmit power does not adjust according to the small-scale channel gains of all the users, the expectation in (24a) is taken over the small-scale channel gain of the  $k$ th user.

Since the left-hand side of the constraint in (24b) is the same as the objective function. We can remove it when solving problem (24). If the minimal bandwidth that is required to guarantee the QoS requirements exceeds  $W_{\max}$ , then problem (24) is infeasible. After removing the constraint in (24b), the bandwidth allocation of the  $k$ th user does not depend on the bandwidth allocation of the other users. Thus, problem (24) can be decomposed into  $K$  single-user problems,

$$\begin{aligned} \min_{W_k} \quad & W_k \\ \text{s.t.} \quad & (23), (24a), W_k > 0, \end{aligned} \tag{25}$$

In the rest part of this section, the index  $k$  is omitted for notational simplicity.

### B. Optimal Bandwidth Allocation for Given $\alpha$

To provide a baseline for the unsupervised deep learning method, in what follows we show how to find the optimal solution with given values of the large-scale channel gain.

Since the achievable rate in (23) increases with  $W$ , the left-hand side of (24a) decreases with  $W$ , and the minimal bandwidth is obtained when the equality in (24a) holds. If effective capacity can be derived as a close-form expression, say for large scale antenna systems [37], then we can use binary search to find the minimal bandwidth. For general wireless systems, where the effective capacity cannot be expressed in a closed form, the constraint in (24a) does not have a closed-form expression. For such kind of problems, the optimal bandwidth allocation can be found with stochastic optimization through the following iterations,

$$W^{(t+1)} = \left[ W^{(t)} + \phi(t) \left( e^{-\vartheta s^{(t)}} - e^{-\vartheta B^E} \right) \right]^+, \tag{26}$$

where  $\phi(t) > 0$  is the step size, and  $s^{(t)}$  is the achievable rate computed from the realization of  $g$  in the  $t$ th iteration according to (23). With the aforementioned assumption (which is true as we validated via simulations) and  $\phi(t) \sim \mathcal{O}(\frac{1}{t})$ ,  $\{W^{(t)}\}$  converges to the unique optimal bandwidth [38].

### C. Learning $W^*(\alpha)$ without Supervision

Since the optimal bandwidth allocation depends on the large-scale channel gains, their relation is denoted by  $W^*(\alpha)$ . With the optimization method in the previous subsection, the system needs to search minimal bandwidth iteratively in every frame. In the sequel we show how to employ unsupervised deep learning to find an approximation of  $W^*(\alpha)$ . According to the analysis in Section II-A, we first transform the bandwidth optimization problem in (25) to the equivalent functional optimization problem,

$$\min_{W(\alpha)} \mathbb{E}_\alpha \{W(\alpha)\} \quad (27)$$

$$\text{s.t. } \mathbb{E}_g \{e^{-\vartheta s(\alpha)}\} - e^{-\vartheta B^E} \leq 0, \quad (27a)$$

$$s(\alpha) = \frac{\tau W(\alpha)}{u \ln 2} \left[ \ln \left( 1 + \frac{\alpha g}{N_0} P_0 \right) - \frac{Q_G^{-1}(\varepsilon_{\max}/2)}{\sqrt{\tau W(\alpha)}} \right], \quad (27b)$$

$$W(\alpha) > 0.$$

Instead of solving the problem in (27), we resort to solving the following problem,

$$\max_{\lambda(\alpha)} \min_{W(\alpha)} L_1 \triangleq \mathbb{E}_\alpha \left\{ W(\alpha) + \lambda(\alpha) \left( \mathbb{E}_g \{e^{-\vartheta s(\alpha)}\} - e^{-\vartheta B^E} \right) \right\} \quad (28)$$

$$\text{s.t. (27b), } W(\alpha) > 0, \lambda(\alpha) > 0, \forall \alpha > 0,$$

where  $\lambda(\alpha)$  is the Lagrange multiplier.

Then, we apply the primal-dual method in Section II-C to solve problem (28). The functions  $W(\alpha)$  and  $\lambda(\alpha)$  are approximated by two fully connected DNNs,  $\hat{W} \triangleq \mathcal{N}_W(\alpha; \boldsymbol{\omega}_W)$  and  $\hat{\lambda} \triangleq \mathcal{N}_\lambda(\alpha; \boldsymbol{\omega}_\lambda)$ , respectively. The approximated objective function in (28) is denoted by  $\hat{L}_1$ , which can be obtained by substituting  $W(\alpha) \approx \hat{W}$  and  $\lambda(\alpha) \approx \hat{\lambda}$  into  $L_1$ . By using `Softplus` as the activation function in the output layers in both DNNs,  $\hat{W}$  and  $\hat{\lambda}$  are positive. The parameters of the DNNs,  $\boldsymbol{\omega}_W$  and  $\boldsymbol{\omega}_\lambda$ , can be obtained iteratively according to the following method,

$$\begin{aligned} \boldsymbol{\omega}_W^{(t+1)} &= \boldsymbol{\omega}_W^{(t)} - \phi(t) \nabla_{\boldsymbol{\omega}_W} \hat{L}_1^{(t)} \\ &= \boldsymbol{\omega}_W^{(t)} - \phi(t) \nabla_{\boldsymbol{\omega}_W} \mathcal{N}_W \left( \alpha^{(t,n)}; \boldsymbol{\omega}_W^{(t)} \right) \frac{d\hat{L}_1^{(t)}}{dW}, \end{aligned} \quad (29)$$

$$\begin{aligned} \boldsymbol{\omega}_\lambda^{(t+1)} &= \boldsymbol{\omega}_\lambda^{(t)} + \phi(t) \nabla_{\boldsymbol{\omega}_\lambda} \hat{L}_1^{(t)} \\ &= \boldsymbol{\omega}_\lambda^{(t)} + \phi(t) \nabla_{\boldsymbol{\omega}_\lambda} \mathcal{N}_\lambda \left( \alpha^{(t,n)}; \boldsymbol{\omega}_W^{(t)} \right) \frac{d\hat{L}_1^{(t)}}{d\lambda}, \end{aligned} \quad (30)$$

where  $\hat{L}_1^{(t)} \triangleq \frac{1}{N_b} \sum_{n=1}^{N_b} \left[ \hat{W}^{(t,n)} + \hat{\lambda}^{(t,n)} \left( e^{-\vartheta \hat{s}^{(t,n)}} - e^{-\vartheta B^E} \right) \right]$  is the realization of  $\hat{L}_1$  in the  $t$ th iteration,  $N_b$  is the number of realizations in each batch<sup>4</sup>,  $\alpha^{(t,n)}$  and  $\hat{s}^{(t,n)}$  are the  $n$ th realizations of the large-scale channel gain and the achievable rate in the  $t$ th iteration, respectively, and  $\hat{W}^{(t,n)} \triangleq \mathcal{N}_W \left( \alpha^{(t,n)}; \boldsymbol{\omega}_W^{(t)} \right)$  and  $\hat{\lambda}^{(t,n)} \triangleq \mathcal{N}_\lambda \left( \alpha^{(t,n)}; \boldsymbol{\omega}_\lambda^{(t)} \right)$ . The gradients of the DNNs w. r. t. the parameters,  $\nabla_{\boldsymbol{\omega}_W} \mathcal{N}_W \left( \alpha^{(t,n)}; \boldsymbol{\omega}_W^{(t)} \right)$  and  $\nabla_{\boldsymbol{\omega}_\lambda} \mathcal{N}_\lambda \left( \alpha^{(t,n)}; \boldsymbol{\omega}_\lambda^{(t)} \right)$ , can be computed by backward propagation, and

$$\begin{aligned} \frac{d\hat{L}_1^{(t)}}{dW} &= 1 - \frac{1}{N_b} \sum_{n=1}^{N_b} \hat{\lambda}^{(t,n)} \vartheta \frac{\partial \hat{s}^{(t,n)}}{\partial \hat{W}} e^{-\vartheta \hat{s}^{(t,n)}}, \\ \frac{d\hat{L}_1^{(t)}}{d\lambda} &= \frac{1}{N_b} \sum_{n=1}^{N_b} \left( e^{-\vartheta \hat{s}^{(t,n)}} - e^{-\vartheta B^E} \right). \end{aligned}$$

From the expression of the achievable rate in (27b), we can derive that

$$\frac{\partial \hat{s}^{(t,n)}}{\partial \hat{W}} = \frac{1}{u \ln 2} \left[ \tau \ln \left( 1 + \frac{\alpha^{(t,n)} g P_0}{N_0} \right) - \frac{Q_G^{-1}(\varepsilon_{\max}/2)}{2} \sqrt{\frac{\tau}{W^{(t,n)}}} \right]. \quad (31)$$

The values of  $B^E$  and  $\vartheta$  are computed according to (18) and (20), respectively.

**Remark 3.** From the above method, we can obtain a well-trained DNN  $\mathcal{N}_W(\alpha; \boldsymbol{\omega}_W)$ . When the  $\alpha$  varies in different frames, the system only needs to compute the bandwidth allocation from  $\mathcal{N}_W(\alpha; \boldsymbol{\omega}_W)$  at the beginning of each frame.

## V. JOINT OPTIMIZATION OF BANDWIDTH ALLOCATION AND POWER CONTROL POLICY

In this section, we show how to exploit multi-user diversity to minimize the total bandwidth required to support the QoS requirement in URLLC by jointly optimizing bandwidth allocation and power control policy. We first obtain the global optimal solution in a special case with the theoretical method introduced in Section II-C. Then, we provide an approximated optimal solution in general cases by resorting to unsupervised deep learning. With the example in this section, we illustrate how to solve a functional optimization problem subject to instantaneous and statistic constraints.

<sup>4</sup>In each iteration, a batch of realizations of large-scale channel gains and estimated bandwidth allocation and Lagrange multipliers will be used to approximate the expectations in (28).

### A. Problem Formulation and Equivalent Transformation

To exploit multi-user diversity, the transmit power allocated to each user is controlled according to the small-scale channel gains of all users  $\mathbf{g}$ . In this way, the transmit power of the BS can be shared among users dynamically in each slot. Adaptively allocating bandwidth according to the small-scale channel gains also yields multi-user diversity, which however can only bring marginal gain as demonstrated in [39]. To reduce the computational complexity, the bandwidth is only allocated to users according to their large-scale channel gains. Nonetheless, the numerical method introduced in Section II-C is still applicable when the bandwidth allocation is also adapted to  $\mathbf{g}$ .

The optimal bandwidth allocation and power control policy that minimizes the total bandwidth required to ensure the QoS of every user can be obtained by solving the following problem,

$$\min_{P_k(\mathbf{g}), W_k} \sum_{k=1}^K W_k \quad (32)$$

$$\text{s.t. } \mathbb{E}_{\mathbf{g}} \{ e^{-\vartheta_k s_k} \} - e^{-\vartheta_k B_k^E} \leq 0, \quad (32a)$$

$$s_k = \frac{\tau W_k}{u \ln 2} \left[ \ln \left( 1 + \frac{\alpha_k g_k P_k(\mathbf{g})}{N_0 W_k} \right) - \frac{Q_G^{-1}(\varepsilon_{\max}/2)}{\sqrt{\tau W_k}} \right], \quad (32b)$$

$$\sum_{k=1}^K P_k(\mathbf{g}) \leq P_{\max}, P_k(\mathbf{g}) \geq 0, W_k \geq 0, \quad (32c)$$

where (32a) is the QoS requirement derived from (21) and (22), (32b) is the achievable packet rate in (15) under the requirement on decoding error probability, and the first term in (32c) is the maximum transmit power constraint. The total bandwidth constraint has been removed from the constraints of problem (32). If the minimal total bandwidth is higher than  $W_{\max}$ , then the problem is infeasible.

Problem (32) involves two timescales. In each slot, the BS adjusts transmit power according to small-scale channel gains. In each frame, the bandwidth allocation is optimized with given large-scale channel gains. As shown in (32a), the power control policy depends on the distribution of the small-scale channel gain, and thus the constraint in (32a) is a statistic constraint. This makes the problem a functional optimization problem.

### B. Optimal Solution in A Symmetric Case

To provide a baseline for the learning-based solution to be introduced later, in what follows we derive the closed-form expression of the optimal solution in a symmetric case, where all

users are located at the cell-edge and have the same arrival process, i.e.,  $\alpha_k = \alpha$  and  $a_k = a$ . Then,  $\vartheta_k = \vartheta$  and both the optimal values of  $W_k$  and  $\kappa_k$  are identical for different  $k$ , i.e.,  $W_k = W$  and  $\kappa_k = \kappa$ .

The Lagrangian of problem (32) can be expressed as follows,

$$L_2 \triangleq \sum_{k=1}^K W_k + \sum_{k=1}^K \kappa_k \left( \mathbb{E}_{\mathbf{g}} \{ e^{-\vartheta_k s_k} \} - e^{-\vartheta_k B_k^E} \right) + \int_{\mathbb{R}_+^K} h(\mathbf{g}) \left( \sum_{k=1}^K P_k(\mathbf{g}) - P_{\max} \right) d\mathbf{g}, \quad (33)$$

where  $h(\mathbf{g})$  and  $\kappa_k$  are the Lagrange multipliers.

Denote the joint pdf of  $\mathbf{g}$  as  $p(\mathbf{g})$ . Then, the optimal solution of problem (32) should satisfy its KKT conditions, which can be derived as [15],

$$\frac{\delta L_2}{\delta P_k(\mathbf{g})} = 0, \quad (34)$$

$$\frac{\partial L_2}{\partial W} = 1 - \kappa \theta \mathbb{E}_{\mathbf{g}} \left\{ \frac{\partial s_k}{\partial W} e^{-\theta s_k} \right\} = 0, \quad (35)$$

$$\kappa_k \left( \mathbb{E}_{\mathbf{g}} \{ e^{-\vartheta_k s_k} \} - e^{-\vartheta_k B_k^E} \right) = 0, \quad (36)$$

$$h(\mathbf{g}) \left( \sum_{k=1}^K P_k(\mathbf{g}) - P_{\max} \right) = 0, \forall \mathbf{g} \in \mathbb{R}_+^K, \quad (37)$$

$$\kappa_k \geq 0, h(\mathbf{g}) \geq 0, \forall \mathbf{g} \in \mathbb{R}_+^K, \quad (38)$$

(32a) and (32c).

By substituting  $L_2$  into (6), we can derive that

$$\frac{\delta L_2}{\delta P_k(\mathbf{g})} = h(\mathbf{g}) - \kappa \theta \frac{\partial s_k}{\partial P_k} e^{-\theta s_k} p(\mathbf{g}). \quad (39)$$

1) *Optimal Power Allocation:* From (34) we have

$$\begin{aligned} h(\mathbf{g}) &= \kappa \theta \frac{\partial s_k}{\partial P_k} e^{-\theta s_k} p(\mathbf{g}) \\ &= \kappa \theta \frac{\tau W}{u \ln 2} \frac{\alpha g_k}{N_0 W} \frac{1}{(1 + \gamma_k)} e^{-\theta s_k} p(\mathbf{g}) \\ &= \frac{\kappa \theta \alpha g_k \tau}{N_0 u \ln 2 (1 + \gamma_k)} (1 + \gamma_k)^{-\frac{\theta W \tau}{u \ln 2}} e^{\frac{\theta \sqrt{W \tau} Q_G^{-1}(\epsilon_{\max}/2)}{u \ln 2}} p(\mathbf{g}) \\ &= \frac{\beta g_k p(\mathbf{g})}{(1 + \gamma_k)^{\frac{1}{\eta}}}, \end{aligned} \quad (40)$$

where  $\gamma_k \triangleq \frac{\alpha g_k P_k(\mathbf{g})}{N_0 W}$  is the SNR of the  $k$ th user,  $\beta \triangleq \frac{\kappa \theta \alpha \tau}{N_0 u \ln 2} e^{\frac{\theta \sqrt{W \tau} Q_G^{-1}(\epsilon_{\max}/2)}{u \ln 2}}$ , and  $\eta \triangleq 1 / (1 + \frac{\theta W \tau}{u \ln 2})$ .

Then, the power allocation function for the  $k$ th user can be derived from (40) as

$$P_k(\mathbf{g}) = \frac{N_0 W}{\alpha g_k} \left[ \left( \frac{\beta g_k p(\mathbf{g})}{h(\mathbf{g})} \right)^\eta - 1 \right]. \quad (41)$$

Since less the required bandwidth to guarantee the QoS requirement decreases with the available transmit power, the optimal solution of problem (32) is obtained when the equality in (32c) hold. Substituting (41) into the equality in the maximum power constraint in (32c), we have

$$\sum_{k=1}^K \frac{N_0 W}{\alpha g_k} \left[ \left( \frac{\beta g_k p(\mathbf{g})}{h(\mathbf{g})} \right)^\eta - 1 \right] = P_{\max}, \quad (42)$$

from which we obtain

$$\left( \frac{\beta p(\mathbf{g})}{h(\mathbf{g})} \right)^\eta = \frac{\frac{\alpha P_{\max}}{N_0 W} + \sum_{k=1}^K g_k^{-1}}{\sum_{k=1}^K g_k^{\eta-1}}. \quad (43)$$

Substituting (42) into (41), we can derive that,

$$P_k(\mathbf{g}) = \frac{N_0 W}{\alpha g_k} \left( \frac{\frac{\alpha g_k P_{\max}}{N_0 W} + g_k \sum_{i=1}^K g_i^{-1}}{g_k^{1-\eta} \sum_{i=1}^K g_i^{\eta-1}} - 1 \right). \quad (44)$$

Further considering that  $P_k(\mathbf{g}) \geq 0$ , the optimal power allocation policy can be obtained as

$$P_k(\mathbf{g}) = \frac{N_0 W}{\alpha g_k} \left( \frac{\frac{\alpha g_k P_{\max}}{N_0 W} + g_k \sum_{i=1}^K g_i^{-1}}{g_k^{1-\eta} \sum_{i=1}^K g_i^{\eta-1}} - 1 \right)^+, \quad (45)$$

which does not depend on the channel distribution  $p(\mathbf{g})$ .

2) *Optimal Bandwidth Allocation:* With the optimal power allocation function, the optimal bandwidth allocated to each user can be found from the equality constraint in (32a). Due to the expectation in (32a) and the complex expression of the achievable rate in (32b), the monotony of (32a) is hard to analyze. Intuitively, the achievable rate should increase with the bandwidth. However, this may not be true when the small-scale channel gain is very small (lower than  $-10$  dB) due to the approximation  $V_k \approx 1$ . Fortunately, since very small values of the small-scale channel gain rarely occur (e.g.,  $\Pr\{g_k < 0.1\} < 10^{-12}$  when  $N_t \geq 8$  for Rayleigh fading channels), the impact can be ignored after taking the expectation. Therefore, it is reasonable to assume that the left-hand side of (32a) decreases with  $W$ . Like (26), the optimal bandwidth allocation can be found with stochastic optimization through the following iterations,

$$W^{(t+1)} = \left[ W^{(t)} + \phi(t) \left( e^{-\vartheta s_k^{(t)}} - e^{-\vartheta B^E} \right) \right]^+, \quad (46)$$

where  $s_k^{(t)}$  is the achievable rate of the  $k$ th user computed from the realization of  $\mathbf{g}$  in the  $t$ th iteration.

**Remark 4.** The KKT conditions are necessary for finding the global optimal solution. Since the power allocation derived from the KKT conditions and the bandwidth allocation found with stochastic optimization to satisfy the KKT condition are unique, the obtained solution is globally optimal.

### C. Solution with Unsupervised Deep Learning in General Cases

In general asymmetric cases, one can hardly derive the closed-form expression of  $P_k(\mathbf{g})$  from the KKT conditions. Since the KKT conditions are partial differential equations, finding the numerical solution is also very challenging. We apply the numerical method in Section II-C to solve problem (32), which can be transformed to the following problem,

$$\begin{aligned} \max_{h(\mathbf{g}), \lambda_k} \min_{P_k(\mathbf{g}), W_k} L_2 \\ \text{s.t. (32b), } P_k(\mathbf{g}) \geq 0, W_k \geq 0, h(\mathbf{g}) \geq 0, \lambda_k \geq 0. \end{aligned} \quad (47)$$

Considering that DNNs are powerful at function learning, we approximate  $P_k(\mathbf{g})$  with a DNN,

$$\left[ \hat{P}_1(\mathbf{g}; \boldsymbol{\omega}_P), \dots, \hat{P}_K(\mathbf{g}; \boldsymbol{\omega}_P) \right]^T = P_{\max} \mathcal{N}(\mathbf{g}; \boldsymbol{\omega}_P), \quad (48)$$

where  $\mathcal{N}_P(\mathbf{g}; \boldsymbol{\omega}_P)$  is a fully connected DNN with inputs  $\mathbf{g}$ , outputs  $\left[ \hat{P}_1(\mathbf{g}; \boldsymbol{\omega}_P), \dots, \hat{P}_K(\mathbf{g}; \boldsymbol{\omega}_P) \right]^T$ , and parameters  $\boldsymbol{\omega}_P$ . As mentioned before (42), the optimal solution of problem (32) is obtained when the equality in (32c) hold. By applying `Softmax` function as the activation function in the output layer, we can guarantee that  $\hat{P}_k(\mathbf{g}; \boldsymbol{\omega}_P) \geq 0$  and  $\sum_{k=1}^K \hat{P}_k(\mathbf{g}; \boldsymbol{\omega}_P) = P_{\max}$ .

Then, we train  $\boldsymbol{\omega}_P$  together with the bandwidth to obtain an approximated optimal resource allocation of the functional optimization problem. We use `ReLU` in the hidden layers as an example activation function, while similar results can be obtained with other activation functions. The width of each hidden layer is set as the number of users. By replacing  $P_k(\mathbf{g})$  in (47) with  $\hat{P}_k(\mathbf{g}; \boldsymbol{\omega}_P)$ , the optimization problem then becomes,

$$\max_{\kappa_k} \min_{\boldsymbol{\omega}_P, W_k} \hat{L}_2 \triangleq \sum_{k=1}^K \left[ W_k + \kappa_k \left( \mathbb{E}_{\mathbf{g}} \left\{ e^{-\vartheta_k \hat{s}_k} \right\} - e^{-\vartheta_k B_k^E} \right) \right] \quad (49)$$

$$\text{s.t. } \hat{s}_k = \frac{\tau W_k}{u \ln 2} \left[ \ln \left( 1 + \frac{\alpha_k g_k \hat{P}_k(\mathbf{g}; \boldsymbol{\omega}_P)}{N_0 W_k} \right) - \frac{Q_G^{-1}(\varepsilon_k^c)}{\sqrt{\tau W_k}} \right], \quad (49a)$$

$$W_k \geq 0, \kappa_k \geq 0.$$

$\sum_{k=1}^K \hat{P}_k(\mathbf{g}; \boldsymbol{\omega}_P) - P_{\max} = 0$  holds when `Softmax` function is applied in the output layer of the DNN. Thus, the term  $\int_{\mathbb{R}_+^K} h(\mathbf{g}) \left( \sum_{k=1}^K P_k(\mathbf{g}) - P_{\max} \right) d\mathbf{g}$  in  $L_2$  disappeared in  $\hat{L}_2$ .

With the primal-dual method, bandwidth allocation,  $W_k$ ,  $k = 1, \dots, K$ , the parameters of the DNN,  $\boldsymbol{\omega}_P$ , and lagrange multipliers,  $\kappa_k$ ,  $k = 1, \dots, K$ , can be obtained iteratively according to the following approach,

$$\begin{aligned} \boldsymbol{\omega}_P^{(t+1)} &= \boldsymbol{\omega}_P^{(t)} - \phi(t) \nabla_{\boldsymbol{\omega}_P} \hat{L}_2^{(t)} \\ &= \boldsymbol{\omega}_P^{(t)} - \phi(t) P_{\max} \nabla_{\boldsymbol{\omega}_P} \mathcal{N}(\mathbf{g}; \boldsymbol{\omega}_P^{(t)}) \nabla_{\hat{\mathbf{P}}} \hat{L}_2^{(t)}, \end{aligned} \quad (50)$$

$$W_k^{(t+1)} = \left[ W_k^{(t)} - \phi(t) \frac{\partial \hat{L}_2^{(t)}}{\partial W_k} \right]^+, \quad (51)$$

$$\begin{aligned} \kappa_k^{(t+1)} &= \left[ \kappa_k^{(t)} + \phi(t) \frac{\partial \hat{L}_2^{(t)}}{\partial \kappa_k} \right]^+ \\ &= \left[ \kappa_k^{(t)} + \phi(t) \frac{1}{N_b} \sum_{n=1}^{N_b} \left( e^{-\theta_k \hat{s}_k^{(t,n)}} - e^{-\theta_k B_k^E} \right) \right]^+, \end{aligned} \quad (52)$$

where  $\hat{L}_2^{(t)} \triangleq \frac{1}{N_b} \sum_{n=1}^{N_b} \sum_{k=1}^K \left[ W_k + \kappa_k \left( e^{-\theta_k \hat{s}_k^{(t,n)}} - e^{-\theta_k B_k^E} \right) \right]$ ,  $\hat{s}_k^{(t,n)}$  is the  $n$ th realization of the achievable rate in the  $t$ th iteration, and  $N_b$  is the batch size in each iteration. The gradient matrix of the DNN with respect to the parameters  $\nabla_{\boldsymbol{\omega}_P} \mathcal{N}(\mathbf{g}; \boldsymbol{\omega}_P^{(t)})$  can be computed through backward propagation, and the gradient  $\hat{L}^{(t)}$  is a column vector, i.e.,

$$\nabla_{\hat{\mathbf{P}}} \hat{L}^{(t)} = \left[ \frac{1}{N_b} \sum_{n=1}^{N_b} \kappa_k^{(t)} \theta_k \frac{\partial \hat{s}_k^{(t,n)}}{\partial \hat{P}_k} e^{-\theta_k \hat{s}_k^{(t,n)}} \right]_{K \times 1}. \quad (53)$$

**Remark 5.** From the iteration of the Lagrange multiplier in (52), we can find that the iteration converges only when the QoS constraint (32a) is satisfied. This means that the QoS requirements can be ensured when the iteration converges.

## VI. SIMULATION RESULTS

In this section, we evaluate the minimal total bandwidth required to ensure the QoS with different policies in both symmetric and asymmetric scenarios.

### A. Simulation Setup

Without lose of generality, we consider a single user case in a single cell with radius of 250 m and path loss model  $10 \lg(\alpha) = 35.3 + 37.6 \lg(d)$ . The simulation setup and fine-tuned hyper-parameters for the neural network are listed in Table I, unless otherwise specified. We use `Softplus` in the output layers in all DNNs, and use `TanH` in the hidden layers as an example activation function.

TABLE I  
SIMULATION PARAMETERS AND HYPER-PARAMETERS

Overall packet loss probability $\varepsilon_{\max}$	$10^{-5}$
Duration of each slot $T_s$	0.1 ms
Duration of DL transmission $\tau$	0.05 ms
DL delay bound $D_{\max}$	10 slots (1 ms)
Transmission delay $D^t$	1 slot [27]
Decoding delay $D^c$	1 slot [27]
Maximal transmit power of BS $P_{\max}$	43 dBm
Path loss model $10 \lg(\alpha)$	$35.3 + 37.6 \lg(d_k)$
Number of antennas $N_t$	8
Single-sided noise spectral density $N_0$	-173 dBm/Hz
Packet size $u$	20 bytes (160 bits) [2]
Average packet arrival rate $a$	0.2 packets/slot
Learning rate $\phi(t)$	$1/(1 + 0.1t)$
Number of hidden layers	2
Batch size $N_b$	100

The cell radius is 250 m. In the symmetric scenario, all users are in the cell-edge. In the asymmetric scenario, the users are uniformly located in a road, where the user-BS distances are from 50 m to 250 m. The small scale channel gains of all users in each slot are randomly generated from Rayleigh distribution, and are independent from those in other slots due to the frequency hopping. Other simulation parameters and fine-tuned hyper-parameters for the DNN are listed in Table I.

The optimal policy (with legend “w MUD w FD”) exploits multi-user diversity by dynamically control the transmit power according the diverse small-scale channel gains of users, and exploits frequency diversity by frequency hopping. The optimal power control policy is obtained from (44) and the optimal bandwidth allocation policy is obtained from (46) with around 200 iterations in the symmetric scenario.

The learning-based optimal power control policy and bandwidth allocation policy are obtained from the iterations in (50), (51) and (52) with random initial values (with legend “w MUD w FD (NN)”). In each slot, the channel realizations in the recent  $N_b$  slots are taken as a batch, which is used for 10 iterations. The training procedure converges after 100 slots, unless otherwise specified.

For comparison, we consider a policy that equally allocates the transmit power to each user without exploiting multi-user diversity, and only optimizes the bandwidth allocation according to the large scale channel gains (with legend “w/o MUD w FD”). In addition, we provide the performance of a heuristic policy in [39], which exploits multi-user diversity by scheduling the users according to the small-scale channel gains of users but does not adopt frequency hopping to exploit frequency diversity (with legend “w MUD w/o FD”). Finally, we show the performance of the policy in [31], which neither exploits multi-user diversity nor frequency diversity (with legend “w/o MUD w/o FD”).

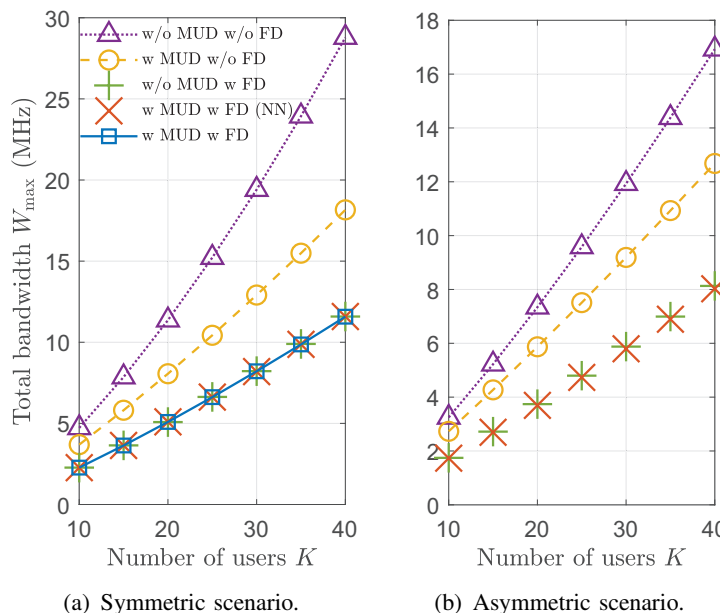


Fig. 2. Total bandwidth required to support the QoS of each user.

In Fig. 2(a), we provide the results in the symmetric scenario. It shows that exploiting multi-user diversity or frequency diversity individually can significantly improve the bandwidth efficiency. However, once the frequency diversity is exploited, multi-user diversity does not provide further improvement. In addition, in this symmetric scenario, the performance of learning-based policy (“w MUD w FD (NN)”) is almost the same as the optimal policy derived in (45) (“w

MUD w FD”).

In Fig. 2(b), we provide the results in the asymmetric scenario. Since the optimal solution is not available in this scenario, we use the learning-based policy to illustrate the performance limit when both multi-user diversity and frequency diversity are available. The gaps among different policies in the asymmetric scenario is similar to that in the symmetric scenario. In addition, the learning-based policy only achieves marginal gains compared with the policy that only exploit frequency diversity (“w/o MUD w FD”). It means that when frequency diversity is exploited, multi-user diversity only provides marginal performance gains.

TABLE II  
NUMBER OF SLOTS FOR CONVERGENCE (ASYMMETRIC SCENARIO)

Convergence percentage	99.9%	99.99%
w/o pre-training	5 000	> 10 000
w pre-training	3	1 000

To show the convergency of the learning-based solution, we consider the absolute sum of the average gradients  $\zeta^{(t)} \triangleq \left\| \mathbb{E}_{\mathbf{g}} \left\{ \nabla_{\omega_P} \hat{L}^{(t)} \right\} \right\|_1 + \sum_{k=1}^K \left| \mathbb{E}_{\mathbf{g}} \left\{ \frac{\partial \hat{L}^{(t)}}{\partial W_k} \right\} \right| + \sum_{k=1}^K \left| \mathbb{E}_{\mathbf{g}} \left\{ \frac{\partial \hat{L}^{(t)}}{\partial \kappa_k} \right\} \right|$  and the average relative error of the QoS constraint  $\xi^{(t)} \triangleq \sum_{k=1}^K \left[ \mathbb{E}_{\mathbf{g}} \left\{ e^{\theta_k (B_k^E - \hat{s}_k^{(t)})} \right\} - 1 \right]^+ / K$ . The training algorithm in (50), (51) and (52) is considered to be converged at the  $t$ th slot when  $\zeta^{(t)} < 1\% \times \sum_{k=1}^K W_k^{(t)}$  and  $\xi^{(t)} < 1\%$ .

The convergence speeds with and without pre-training are shown in Table II, which are obtained from 100 000 simulations. In each simulation, 40 users are randomly dropped on the road. For the results without pre-training, the parameters are trained with random initial values until convergence, which needs 10 000 slots (i.e., 1 s) for 99.99% convergence. For the results with pre-training, all users move at 72 kph along the road in the same direction, and the parameters are retrained every 0.1 s by taking the pre-trained parameters as the initial values. We can see that the pre-training can significantly shorten the convergence time, which can be done off-line.

The complexity of the training algorithm is low. A computer with Intel® Core™ i7-6700 CPU is able to finish around 1 000 iterations in 0.1 s without using the acceleration from GPU.

## VII. CONCLUSION

In this paper, we proposed an approach of using unsupervised deep learning to solve functional optimization problems with both instantaneous and long-term constraints. We considered two example problems in downlink URLLC. In the first problem, we optimized the bandwidth allocation according to the large-scale channel gain, where an instantaneous constraint on total bandwidth is considered. In the second problem, we further optimized instantaneous power according to small-scale channel gains, where a long-term constraint on the power control policy is considered. To illustrate how to solve a functional optimization problem, we derived the closed-form expression of the optimal power control policy in a symmetric scenario. Furthermore, the unsupervised deep learning method was introduced to find the approximated optimal solution in asymmetric scenarios. Simulation results showed that the learning-based solution can achieve the same performance with the optimal solution in the symmetric scenario. The training algorithm is with low computational complexity and converges rapidly with pre-training. Besides, we also illustrated how to improve the bandwidth utilization efficiency of URLLC by exploiting frequency diversity and multi-user diversity.

## APPENDIX A

### PROOF OF THE EQUIVALENCE BETWEEN PROBLEMS (1) AND (2)

*Proof.* We first proof that any optimal solutions of problem (1) are optimal for problem (2). Denote  $\mathbf{x}^*(\boldsymbol{\theta}_1)$  as an optimal solution of problem (1) given an arbitrary realization  $\boldsymbol{\theta}_1 \in \mathcal{D}_\theta$ , and denote the objective function in (2) as  $\mathcal{F}[\mathbf{x}(\boldsymbol{\theta})] \triangleq \int_{\boldsymbol{\theta} \in \mathcal{D}_\theta} f[\mathbf{x}(\boldsymbol{\theta}); \boldsymbol{\theta}] p(\boldsymbol{\theta}) d\boldsymbol{\theta}$ . Let  $\mathbf{x}_1(\boldsymbol{\theta}), \boldsymbol{\theta} \in \mathcal{D}_\theta$  be an arbitrary feasible solution of problem (2). Since problems (1) and (2) have the same constraints, they have the same feasible region. Thus,  $\mathbf{x}_1(\boldsymbol{\theta}_1)$  is a feasible solution of problem (1). Given the realization  $\boldsymbol{\theta}_1$ , the optimal solution of problem (1) is better than any feasible solutions of problem (1), i.e.,

$$f[\mathbf{x}^*(\boldsymbol{\theta}_1); \boldsymbol{\theta}_1] - f[\mathbf{x}_1(\boldsymbol{\theta}_1); \boldsymbol{\theta}_1] \leq 0, \quad \forall \boldsymbol{\theta}_1 \in \mathcal{D}_\theta. \quad (\text{A.1})$$

Since  $p(\boldsymbol{\theta}) \geq 0$ , we further have,

$$\mathcal{F}[\mathbf{x}^*(\boldsymbol{\theta})] - \mathcal{F}[\mathbf{x}_0(\boldsymbol{\theta})] = \int_{\boldsymbol{\theta} \in \mathcal{D}_\theta} [f[\mathbf{x}^*(\boldsymbol{\theta}); \boldsymbol{\theta}] - f[\mathbf{x}_0(\boldsymbol{\theta}); \boldsymbol{\theta}]] p(\boldsymbol{\theta}) d\boldsymbol{\theta} \leq 0. \quad (\text{A.2})$$

Since  $\mathbf{x}^*(\boldsymbol{\theta}), \boldsymbol{\theta} \in \mathcal{D}_\theta$ , satisfies all the constraints in problem (2), it is a feasible solution of problem (2). (A.2) indicates that  $\mathbf{x}^*(\boldsymbol{\theta}), \boldsymbol{\theta} \in \mathcal{D}_\theta$ , is better than an arbitrary solution of problem (2). Thus, it is optimal for problem (2).

In what follows, we proof that optimal solutions of problem (2) are optimal for problem (1) with probability one. We denote an optimal solution of problem (2) by  $\mathbf{x}_{\text{opt}}(\boldsymbol{\theta}), \boldsymbol{\theta} \in \mathcal{D}_\theta$ , and denote an optimal solution of problem (1) with parameter  $\boldsymbol{\theta}$  by  $\mathbf{x}^*(\boldsymbol{\theta})$ . Then,

$$f[\mathbf{x}_{\text{opt}}(\boldsymbol{\theta}); \boldsymbol{\theta}] - f[\mathbf{x}^*(\boldsymbol{\theta}), \boldsymbol{\theta}] \geq 0, \quad \forall \boldsymbol{\theta} \in \mathcal{D}_\theta. \quad (\text{A.3})$$

Suppose there exists a non-zero measure set,  $\mathcal{D}_\theta^+$ , such that for any  $\boldsymbol{\theta}' \in \mathcal{D}_\theta^+$ ,  $\mathbf{x}_{\text{opt}}(\boldsymbol{\theta}')$  is not optimal for problem (1). In other words, there exists a  $\delta_0$  such that

$$f[\mathbf{x}_{\text{opt}}(\boldsymbol{\theta}'); \boldsymbol{\theta}'] - f[\mathbf{x}^*(\boldsymbol{\theta}'), \boldsymbol{\theta}'] \geq \delta_0 > 0, \quad \forall \boldsymbol{\theta}' \in \mathcal{D}_\theta^+. \quad (\text{A.4})$$

Here, a non-zero measure set is a set that  $\Pr\{\boldsymbol{\theta}' \in \mathcal{D}_\theta^+\} > 0$ .

From (A.3) and (A.4), we can derive that

$$\begin{aligned} & \mathcal{F}[\mathbf{x}_{\text{opt}}(\boldsymbol{\theta})] - \mathcal{F}[\mathbf{x}^*(\boldsymbol{\theta})] \\ &= \int_{\boldsymbol{\theta} \in \mathcal{D}_\theta} [f[\mathbf{x}_{\text{opt}}(\boldsymbol{\theta}); \boldsymbol{\theta}] - f[\mathbf{x}^*(\boldsymbol{\theta}), \boldsymbol{\theta}]] p(\boldsymbol{\theta}) d\boldsymbol{\theta} \\ &\geq \int_{\boldsymbol{\theta} \in \mathcal{D}_\theta^+} [f[\mathbf{x}_{\text{opt}}(\boldsymbol{\theta}); \boldsymbol{\theta}] - f[\mathbf{x}^*(\boldsymbol{\theta}), \boldsymbol{\theta}]] p(\boldsymbol{\theta}) d\boldsymbol{\theta} \\ &\geq \int_{\boldsymbol{\theta} \in \mathcal{D}_\theta^+} \delta_0 p(\boldsymbol{\theta}) d\boldsymbol{\theta} \\ &= \delta_0 \Pr\{\boldsymbol{\theta} \in \mathcal{D}_\theta^+\} > 0, \end{aligned} \quad (\text{A.5})$$

This contradicts with the definition that  $\mathbf{x}_{\text{opt}}(\boldsymbol{\theta})$  is the optimal solution of problem (2). Therefore, the optimal solutions of problem (2) are optimal for problem (1) with probability one. This completes the proof.  $\square$

## APPENDIX B

### THE METHOD TO COMPUTE (12), (13) AND (14)

*Proof.* For notational simplicity, we omitted the index of iteration  $t$  in this appendix. To compute (12), (13) and (14), we only need to compute  $\nabla_{\omega_x} \hat{L}$ ,  $\nabla_{\omega_\lambda} \hat{L}$  and  $\partial \hat{L} / \partial \nu_j$ .

The value of  $\nabla_{\omega_x} \hat{L}$  can be obtained from the following expression,

$$\begin{aligned} \nabla_{\omega_x} \hat{L} &= \int_{\boldsymbol{\theta} \in D_{\theta}} [\nabla_{\omega_x} \hat{\boldsymbol{x}}(\boldsymbol{\theta})] [\nabla_{\hat{\boldsymbol{x}}(\boldsymbol{\theta})} f(\hat{\boldsymbol{x}}(\boldsymbol{\theta}); \boldsymbol{\theta})] p(\boldsymbol{\theta}) d\boldsymbol{\theta} \\ &+ \sum_{j=I+1}^J \nu_j \int_{\boldsymbol{\theta} \in D_{\theta}} [\nabla_{\omega_x} \hat{\boldsymbol{x}}(\boldsymbol{\theta})] [\nabla_{\hat{\boldsymbol{x}}(\boldsymbol{\theta})} C_j(\hat{\boldsymbol{x}}(\boldsymbol{\theta}); \boldsymbol{\theta})] p(\boldsymbol{\theta}) d\boldsymbol{\theta} \\ &+ \sum_{i=1}^I \int_{\boldsymbol{\theta} \in D_{\theta}} \hat{\lambda}_i(\boldsymbol{\theta}) [\nabla_{\omega_x} \hat{\boldsymbol{x}}(\boldsymbol{\theta})] [\nabla_{\hat{\boldsymbol{x}}(\boldsymbol{\theta})} C_i(\hat{\boldsymbol{x}}(\boldsymbol{\theta}); \boldsymbol{\theta})] d\boldsymbol{\theta}, \end{aligned} \quad (\text{B.1})$$

where  $\nabla_{\omega_x} \hat{\boldsymbol{x}}(\boldsymbol{\theta}) \triangleq [\nabla_{\omega_x} \hat{x}_1(\boldsymbol{\theta}), \dots, \nabla_{\omega_x} \hat{x}_{N_x}(\boldsymbol{\theta})]$  can be obtained via backward propagation.

The values of  $\nabla_{\omega_{\lambda}} \hat{L}$  and  $\partial \hat{L} / \partial \nu_j$  can be obtained from

$$\nabla_{\omega_{\lambda}} \hat{L} = \sum_{i=1}^I \int_{\boldsymbol{\theta} \in D_{\theta}} [\nabla_{\omega_{\lambda}} \hat{\lambda}_i(\boldsymbol{\theta})] [C_i(\hat{\boldsymbol{x}}(\boldsymbol{\theta}); \boldsymbol{\theta})] d\boldsymbol{\theta}, \quad (\text{B.2})$$

$$\frac{\partial \hat{L}}{\partial \nu_j} = \int_{\boldsymbol{\theta} \in D_{\theta}} C_j(\hat{\boldsymbol{x}}(\boldsymbol{\theta}); \boldsymbol{\theta}) p(\boldsymbol{\theta}) d\boldsymbol{\theta}, \quad (\text{B.3})$$

where  $\nabla_{\omega_{\lambda}} \hat{\lambda}_i(\boldsymbol{\theta}), i = 1, \dots, I$ , can be obtained via backward propagation.  $\square$

## REFERENCES

- [1] C. Sun and C. Yang, "Unsupervised deep learning for ultra-reliable and low-latency communications," in *Proc. IEEE Globecom*, 2019.
- [2] 3GPP, *Study on Scenarios and Requirements for Next Generation Access Technologies*. Technical Specification Group Radio Access Network, Technical Report 38.913, Release 14, Oct. 2016.
- [3] C. She, R. Dong, Z. Gu, Z. Hou, Y. Li, W. Hardjawana, C. Yang, L. Song, and B. Vucetic, "Deep learning for ultra-reliable and low-latency communications in 6g networks," *IEEE Network*, *accepted*, 2020.
- [4] N. P. Osmolovskii, *Calculus of variations and optimal control*. American Mathematical Soc., 1998, vol. 180.
- [5] O. C. Zienkiewicz, R. L. Taylor, P. Nithiarasu, and J. Zhu, *The finite element method*. McGraw-hill London, 1977, vol. 3.
- [6] D. Liu, C. Sun, C. Yang, and L. Hanzo, "Optimizing wireless systems using unsupervised and reinforced-unsupervised deep learning," *IEEE Network*, *early access*, 2020.
- [7] K. Hornik, M. B. Stinchcombe, and H. White, "Multilayer feedforward networks are universal approximators," *Neural Networks*, vol. 2, no. 5, pp. 359–366, 1989.
- [8] H. Sun, X. Chen, Q. Shi, M. Hong, X. Fu, and N. D. Sidiropoulos, "Learning to optimize: Training deep neural networks for interference management," *IEEE Trans. on Signal Proc.*, vol. 66, no. 20, pp. 5348–5453, Oct. 2018.
- [9] J. Guo and C. Yang, "Predictive resource allocation with deep learning," in *IEEE VTC Fall*, 2018.
- [10] L. Liu, B. Yin, S. Zhang, X. Cao, and Y. Cheng, "Deep learning meets wireless network optimization: Identify critical links," *IEEE Trans. Network Science and Engineering*, pp. 1–1, 2018.

- [11] R. Dong, C. She, W. Hardjawana, Y. Li, and B. Vucetic, “Deep learning for radio resource allocation with diverse quality-of-service requirements in 5G,” *arXiv preprint arXiv:2004.00507*, 2020.
- [12] N. Ben-Khalifa, M. Assaad, and M. Debbah, “Risk-sensitive reinforcement learning for URLLC traffic in wireless networks,” *arXiv preprint arXiv:1811.02341*, 2018.
- [13] A. Elgabli, H. Khan, M. Krouka, and M. Bennis, “Reinforcement learning based scheduling algorithm for optimizing age of information in ultra reliable low latency networks,” *arXiv preprint arXiv:1811.06776*, 2018.
- [14] A. Goldsmith, *Wireless Communications*. Cambridge University Press, 2005.
- [15] J. Gregory, *Constrained optimization in the calculus of variations and optimal control theory*. Chapman and Hall/CRC, 2018.
- [16] A. Sasane, *Calculus of Variations and Optimal Control*, 2014. [Online]. Available: <https://epdf.pub/calculus-of-variations-amp-optimal-control.html>
- [17] S. Boyd and L. Vandenberghe, *Convex Optimization*. Cambridge University Press, 2004.
- [18] D. G. Luenberger, *Optimization by vector space methods*. John Wiley & Sons, 1997.
- [19] H. Sun, X. Chen, Q. Shi, M. Hong, X. Fu, and N. D. Sidiropoulos, “Learning to optimize: Training deep neural networks for interference management,” *IEEE Trans. Signal Process.*, vol. 66, no. 20, pp. 5438–5453, Oct. 2018.
- [20] M. Eisen, C. Zhang, L. F. O. Chamon, D. D. Lee, and A. Ribeiro, “Learning optimal resource allocations in wireless systems,” *IEEE Trans. Signal Process.*, vol. 67, no. 10, pp. 2775–2790, May 2019.
- [21] H. Lee, S. H. Lee, and T. Q. S. Quek, “Deep learning for distributed optimization: Applications to wireless resource management,” *IEEE J. Sel. Areas in Commun.*, *accepted*, 2019.
- [22] V. Nair and G. E. Hinton, “Rectified linear units improve restricted boltzmann machines,” in *Proc. ICML*, 2010, pp. 807–814.
- [23] X. Glorot, A. Bordes, and Y. Bengio, “Deep sparse rectifier neural networks,” in *Proc. AISTATS*, 2011, pp. 315–323.
- [24] C. She, C. Yang, and T. Q. S. Quek, “Joint uplink and downlink resource configuration for ultra-reliable and low-latency communications,” *IEEE Trans. Commun.*, vol. 66, no. 5, pp. 2266–2280, May 2018.
- [25] G. Zhang, T. Q. S. Quek, M. Kountouris, *et al.*, “Fundamentals of heterogeneous backhaul design—analysis and optimization,” *IEEE Trans. Commun.*, vol. 64, no. 2, pp. 876–889, Feb. 2016.
- [26] B. Makki, T. Svensson, G. Caire, and M. Zorzi, “Fast HARQ over finite blocklength codes: A technique for low-latency reliable communication,” *IEEE Trans. on Wireless Commun.*, vol. 18, no. 1, pp. 194–209, Jan 2019.
- [27] M. Condoluci, T. Mahmoodi, E. Steinbach, and M. Dohler, “Soft resource reservation for low-delayed teleoperation over mobile networks,” *IEEE Access*, vol. 5, pp. 10 445–10 455, May 2017.
- [28] 3GPP TR 38.802 V2.0.0, “Study on new radio (NR) access technology; physical layer aspects (release 14),” Sep. 2017.
- [29] S. Schiessl, J. Gross, and H. Al-Zubaidy, “Delay analysis for wireless fading channels with finite blocklength channel coding,” in *ACM MSWiM*, 2015.
- [30] W. Yang, G. Durisi, T. Koch, *et al.*, “Quasi-static multiple-antenna fading channels at finite blocklength,” *IEEE Trans. Inf. Theory*, vol. 60, no. 7, pp. 4232–4264, Jul. 2014.
- [31] C. She, C. Yang, and T. Q. S. Quek, “Cross-layer optimization for ultra-reliable and low-latency radio access networks,” *IEEE Trans. Wireless Commun.*, vol. 17, no. 1, pp. 127–141, Jan 2018.
- [32] C. Chang and J. A. Thomas, “Effective bandwidth in high-speed digital networks,” *IEEE J. Sel. Areas Commun.*, vol. 13, no. 6, pp. 1091–1100, Aug. 1995.
- [33] D. Wu and R. Negi, “Effective capacity: a wireless link model for support of quality of service,” *IEEE Transactions on Wireless Communications*, vol. 2, no. 4, pp. 630–643, July 2003.

- [34] J. Tang and X. Zhang, “Quality-of-service driven power and rate adaptation over wireless links,” *IEEE Trans. on Wireless Commun.*, vol. 6, no. 8, pp. 3058–3068, August 2007.
- [35] L. Liu, P. Parag, J. Tang, W. Y. Chen, and J. F. Chamberland, “Resource allocation and quality of service evaluation for wireless communication systems using fluid models,” *IEEE Trans. on Inf. Theory*, vol. 53, no. 5, pp. 1767–1777, May 2007.
- [36] 3GPP, *LTE; E-UTRA; Physical layer procedures*. TS 36.213 v. 8.8.0 Release 8, Oct. 2009.
- [37] C. She, C. Yang, and L. Liu, “Energy-efficient resource allocation for MIMO-OFDM systems serving random sources with statistical QoS requirement,” *IEEE Trans. on Commun.*, vol. 63, no. 11, pp. 4125–4141, Nov 2015.
- [38] L. Bottou, “Online algorithms and stochastic approximations,” in *Online Learning and Neural Networks*, D. Saad, Ed. Cambridge, UK: Cambridge University Press, 1998, revised, Oct. 2012. [Online]. Available: <http://leon.bottou.org/papers/bottou-98x>
- [39] C. Sun, C. She, and C. Yang, “Exploiting multi-user diversity for ultra-reliable and low-latency communications,” in *IEEE Globecom Workshops*, 2017.